Biomaterials 34 (2013) 7269–7280

Contents lists available at SciVerse ScienceDirect

Biomaterials

journal homepage: www.elsevier.com/locate/biomaterials

Off-the-shelf human decellularized tissue-engineered heart valves in a non-human primate model

Benedikt Weber [a,b,c,1], Petra E. Dijkman [d,1], Jacques Scherman [c,e,f,1], Bart Sanders [d], Maximilian Y. Emmert [a,b,c], Jürg Grünenfelder [b,c], Renier Verbeek [e,f], Mona Bracher [f], Melanie Black [f], Thomas Franz [e,f,g], Jeroen Kortsmit [e,f], Peter Modregger [h,i], Silvia Peter [h,j], Marco Stampanoni [h,j], Jérôme Robert [a,b], Debora Kehl [a,b], Marina van Doeselaar [d], Martin Schweiger [a,b,c], Chad E. Brokopp [a,b], Thomas Wälchli [a,b,k], Volkmar Falk [b,c], Peter Zilla [e,f], Anita Driessen-Mol [d], Frank P.T. Baaijens [d], Simon P. Hoerstrup [a,b,c,d,*]

[a] Swiss Center of Regenerative Medicine, University of Zürich, Moussonstrasse 13, CH-8091 Zürich, Switzerland
[b] Division of Surgical Research, University Hospital of Zurich, Raemistrasse 100, CH-8091 Zürich, Switzerland
[c] Clinic for Cardiovascular Surgery, University Hospital of Zurich, Moussonstrasse 13, CH-8091 Zürich, Switzerland
[d] Department of Biomedical Engineering, Soft Tissue Biomechanics and Tissue Engineering, Eindhoven University of Technology, P.O. Box 513, 5600 MB Eindhoven, The Netherlands
[e] Chris Barnard Division of Cardiothoracic Surgery, Groote Schuur Hospital, University of Cape Town, South Africa
[f] Cardiovascular Research Unit, Cape Heart Centre, University of Cape Town, South Africa
[g] Programme for the Enhancement of Research Capacity, Research Office, University of Cape Town, Mowbray, South Africa
[h] Swiss Light Source, Paul Scherrer Institute, 5232 Villigen, Switzerland
[i] University of Lausanne, School of Biology and Medicine, Rue du Bugnon 21, CH-1015 Lausanne, Switzerland
[j] Institute for Biomedical Engineering, University and ETH Zurich, ETZ-F-85, Gloriastrasse 35, 8092 Zurich, Switzerland
[k] Department of Health Sciences and Technology, Swiss Federal Institute of Technology Zurich, CH-8057 Zurich, Switzerland

ARTICLE INFO

Article history:
Received 18 April 2013
Accepted 27 April 2013
Available online 28 June 2013

Keywords:
Heart valve tissue engineering
Tissue regeneration
Decellularization
Preclinical in vivo model
Minimally invasive
Homologous valve replacement

ABSTRACT

Heart valve tissue engineering based on decellularized xenogenic or allogenic starter matrices has shown promising first clinical results. However, the availability of healthy homologous donor valves is limited and xenogenic materials are associated with infectious and immunologic risks. To address such limitations, biodegradable synthetic materials have been successfully used for the creation of living autologous tissue-engineered heart valves (TEHVs) in vitro. Since these classical tissue engineering technologies necessitate substantial infrastructure and logistics, we recently introduced decellularized TEHVs (dTEHVs), based on biodegradable synthetic materials and vascular-derived cells, and successfully created a potential off-the-shelf starter matrix for guided tissue regeneration. Here, we investigate the host repopulation capacity of such dTEHVs in a non-human primate model with up to 8 weeks follow-up. After minimally invasive delivery into the orthotopic pulmonary position, dTEHVs revealed mobile and thin leaflets after 8 weeks of follow-up. Furthermore, mild-moderate valvular insufficiency and relative leaflet shortening were detected. However, in comparison to the decellularized human native heart valve control – representing currently used homografts – dTEHVs showed remarkable rapid cellular repopulation. Given this substantial in situ remodeling capacity, these results suggest that human cell-derived bioengineered decellularized materials represent a promising and clinically relevant starter matrix for heart valve tissue engineering. These biomaterials may ultimately overcome the limitations of currently used valve replacements by providing homologous, non-immunogenic, off-the-shelf replacement constructs.

1. Introduction

In spite of the major advances with regard to minimally invasive catheter-based approaches, valvular heart disease remains to be a significant global health problem with increasing morbidity and mortality in the developing world as well as industrialized countries

* Corresponding author. Swiss Center for Regenerative Medicine, University of Zurich, Moussonstrasse 13, 8091 CH-Zürich, Switzerland. Tel.: +41 44 255 3644; fax: +41 44 255 43.
E-mail address: simon_philipp.hoerstrup@usz.ch (S.P. Hoerstrup).
[1] These authors contributed equally to the paper.

0142-9612/$ – see front matter © 2013 Elsevier Ltd. All rights reserved.
http://dx.doi.org/10.1016/j.biomaterials.2013.04.059

[1,2]. Although the currently available heart valve replacement procedures change the universal fatal outcomes of valvular heart disease, prosthesis-related complications are reported in up to 50% of prosthetic heart valve recipients within 12 years after the operation [3]. While mechanical, metal-based prostheses require lifelong anticoagulation therapy as they are inherently prone to thromboembolic complications, bioprosthetic substitutes undergo progressive calcification and structural deterioration [4,5]. In addition, none of the currently used non-viable valve substitutes hold the potential for regeneration and growth [6].

Striving for improvement of these suboptimal materials in clinical use, decellularized xenogenic or allogenic heart valves have been used as starter matrices for tissue-engineering of valve replacements with promising (pre-)clinical results [6–8]. However, xenogenic grafts are associated with the risk of immunogenic reactions as well as zoonotic disease transmission [9,10] and the availability of homografts is limited [11]. Therefore, biodegradable synthetic materials have been successfully used for the fabrication of fully autologous tissue-engineered heart valves (TEHVs) [12,13]. These living autologous heart valve substitutes with regeneration and growth potential could potentially overcome the limitations of the available heart valve prostheses in clinical use. In recent studies we demonstrated the principal feasibility of merging autologous cell-based heart valve tissue engineering procedures and minimally invasive delivery methods in the ovine [14–16] as well as the senescent non-human primate model [17], which extended the spectrum of tissue engineering to transcatheter heart valve replacement. However, although these initial experiences were promising and demonstrated first in vivo functionality of minimally invasive bioengineered heart valves, autologous cell-based living TEHVs are associated with substantial and almost prohibitive technological and logistical complexity, also involving regulatory approval of ex-vivo cell processing procedures [18].

Therefore, decellularized TEHVs based on biodegradable synthetic materials and homologous cells have been recently developed as potential 'off-the-shelf' alternatives [19]. These constructs combine major advantages of apparent technologies: i) they represent human cell-derived starter matrices for guided tissue regeneration and host cell repopulation and may harbor the advantages of (living) bioengineered constructs – such as regeneration and growth; ii) they would provide homologous (non-xenogenic) replacement structures lacking the risk of zoonotic disease transmission; and iii) they could be produced as 'off-the-shelf' constructs and may principally offer an unlimited supply of valvular replacement structures.

The present study investigates the implantation of human cell-derived decellularized tissue-engineered heart valves (dTEHVs) using minimally invasive implantation techniques in a senescent non-human primate model. Although most previous tissue engineering in vivo investigations have focused on the sheep preclinical animal model (as also requested by some regulatory authorities), recent studies revealed that the significance of the results obtained in the ovine model may be limited given the species-specific remodeling response different to a human-like cardiovascular environment. In contrast, recent experiments suggest that the non-human primate model displays a more appropriate and predictive preclinical model, in particular with regard to endogenous cell repopulation and (neo-)tissue formation, thereby representing an important step prior to the clinical translation of the tissue engineering technologies [17].

2. Materials and methods

2.1. TEHV scaffold fabrication

Trileaflet heart valve scaffolds ($n = 8$) were fabricated as previously described [16,19]. Briefly, scaffolds made from non-woven polyglycolic-acid meshes (PGA; thickness 1.0 mm; specific gravity 70 mg/cm^3; Cellon, Bereldange, Luxembourg) were integrated into radially self-expandable nitinol stents (length = 30.0 mm; OD = 20.0 mm; pfm-AG, Köln, Germany) by using single interrupted sutures (Polypropylene, Ethicon, USA) and coated with 1% poly-4-hydroxybutyrate (MW 1×10^6; P4HB; TEPHA Inc., Lexington, MA, USA) in tetrahydrofuran solution (THF; Sigma Aldrich, St. Louis, MO, USA). After solvent evaporation and vacuum drying overnight, the scaffolds were placed into a 70% EtOH (70% ethanol absolute (VWR international S.A.S. Fontenay-Sous-Bois, France) and 30% autoclaved ultrapure water) twice for 15 min to obtain sterility. Thereafter, scaffolds were incubated for 30 min at 37 °C in PBS (Sigma Aldrich Inc., USA) supplemented with 10% Penicillin-streptomycin (Lonza, Verviers Belgium) and 50 μg/ml Fungin (Invitrogen, San Diego, USA), followed by two washing cycles with PBS.

2.2. Isolation of human fibroblasts

Human vascular-derived cells were harvested by plating from the human vena saphena magna of a 77-year-old patient, according to the Dutch guidelines for secondary used materials. Cells were expanded up to the sixth passage using standard cell culture methods in a humidified atmosphere containing 5% CO_2 at 37 °C. Culture medium consisted of DMEM advanced (Gibco, Invitrogen, Carlsbad, USA), supplemented with 10% Fetal Bovine Serum (FBS; Gibco, Invitrogen), 1% GlutaMax (Gibco, Invitrogen), and 1% penicillin-streptomycin (Lonza, Verviers Belgium).

2.3. Phenotyping of human fibroblasts

Isolated cells were characterized using immunofluorescence staining. Primary antibodies used for characterization of cells were against α-smooth muscle actin (mM-anti-human, clone 1A4, DakoCytomation, Copenhagen, Denmark), desmin (mM-anti-human desmin, clone D33, DakoCytomation), vimentin (mM-anti-human vimentin, clone Vim 3B4, DakoCytomation), and CD45 (mM-anti-human CD45, clone HI30, Biolegend). Alexa 546 phalloidin (A22283, Invitrogen Corp., USA) and DAPI (AD8417, Sigma Co., USA) were used as control staining. Primary antibodies were detected with Cyanine-2 goat-anti-mouse (Jackson Immunoresearch Laboratories Inc., West Grove, PA).

For immunostainings cells were first washed with PBS and then fixed with 4% paraformaldehyde in PBS for 10 min. Following a second washing phase (PBS), they were blocked and permeabilized in 0.2% Triton X-100 (Sigma) in PBS for 10 min. After blocking with 5% goat serum and 1% bovine serum albumin in PBS for 30 min, primary antibodies were added and incubated for 1 h at room temperature. After three washing steps with PBS for 5 min, secondary antibodies were added and incubated for 45 min. The specimens were washed again three times in PBS for 5 min and mounted in Aqua-Poly/Mount™. Analysis of the stained sections and cells was carried out using an inverted fluorescence microscope equipped with a CCD camera (ZEISS Axiovert 40 CFL and ZEISS Axioplan II; Carl Zeiss AG, Oberkochen, Germany). Image processing was performed using the ZEISS AxioVision™ software (Carl Zeiss AG) and the Office Picture Manager (Microsoft Inc., USA).

2.4. Heart valve tissue engineering

Isolated human fibroblasts were expanded up to passage six and were seeded (1.5×10^6 cells/cm^2) onto stented heart valve scaffolds ($n = 8$) using fibrin as a cell carrier [20]. After seeding and static pre-incubation, the constructs were placed into a diastolic pulse duplicator system for culture in closed configuration [21]. The TE-medium (DMEM Advanced, supplemented with 0.1% lamb serum, 1% GlutaMax, 1% Penicillin-streptomycin, and Lascorbic acid 2-phosphate (0.25 mg/ml; Sigma–Aldrich)) was replaced every 2–3 days. The leaflets were exposed to dynamic strains by applying increasing transvalvular pressure differences that started from 3 mm Hg after 5 days and build up to 15 mm Hg in the 4 following days and kept as such until the fourth week.

2.5. Decellularization

After 4 weeks of dynamic conditioning the in vitro grown TEHVs ($n = 8$) were decellularized using the previously described decellularization protocol [19]. Briefly, the TEHVs were washed three times in PBS (Sigma Aldrich) and incubated overnight in PBS supplemented with 0.25% Triton X-100, 0.25% sodium deoxycholate (SD, Sigma–Aldrich), and 0.02% EDTA (Sigma Aldrich) at 37 °C followed by two washing cycles in PBS. Next, the TEHVs were treated with a nuclease digestion solution of 50-mM TRIS-HCI buffer (Tris (hydroxymethyl)-aminomethane (Merck) pH 8.0, supplemented with 100 U/mL Benzonase® (25 units/μl, Novagen, Madison WI USA) and 1 mmol/l of $MgCl_2$ (Merck)) at 37 °C to remove remaining nucleic remnants. After 5–8 h the nuclease digestion solution was replaced with a nuclease digestion solution supplemented with 80 U/mL Benzonase® and incubated overnight. Thereafter, the solution was replaced again by a 20 U/mL Benzonase® solution and incubated for 5–8 h. The valves were washed twice in PBS followed by a washing cycle with M-199 medium (Gibco, Invitrogen Inc.) for more than 24 h at 4 °C to remove cellular remnants. Subsequently, the valves were incubated for 30 min at 37 °C in PBS supplemented with 10% Penicillin-streptomycin and 50 μg/ml Fungin, sterilized in 70% EtOH for 15 min, and again washed twice in PBS. All steps were conducted under continuous shaking. Decellularized TEHVs (dTEHVs) were stored in fresh M-199

medium (at 4 °C) until implantation ($n = 6$) or analysis as controls of the implants ($n = 2$).

In addition to the dTEHV, two decellularized human native heart valves (dHNHVs) were included in the study to serve as a control group, representing clinically used homografts. These dHNHVs were fabricated by integrating human cryopreserved native heart valve matrices into nitinol stents, in a similar way as the TEHV scaffolds, and decellularized using a trypsin-EDTA-based incubation technique. Shortly, after washing the cryopreserved human valves for 1 h in iodine solution and PBS, the valves were placed into an antibiotic solution (containing amikacin (Bristol-Myers Quibb, Switzerland), flucytosin (MEDA Pharmaceuticals, Switzerland), vancomycin (Sandoz Pharmaceuticals, Switzerland), ciprofloxacin (Fresenius Kabi, Switzerland), and metronidazole (Sanofi-aventis, Switzerland)) for 12 h at 4 °C. The next 12 h, the valves were incubated in a solution of 0.05% trypsin-EDTA (Gibco Life Technologies Inc.) at 37 °C and 5% CO_2 under continuous 3D-shaking. This was followed by a washing in PBS for 24 h to remove dead cells and cellular detritus. Finally, the dHNHVs were transferred to PBS for storage prior to implantation.

2.6. Tissue-engineered heart valve implantation and in vivo functionality

For evaluation of the in vivo functionality and host repopulation in non-human primates (chacma baboons), dTEHVs ($n = 6$) and dHNHV ($n = 1$) were minimally invasively implanted into the orthotopic pulmonary valve position as meticulously described before [16,17]. Briefly, a mini-sternotomy was performed and the valves were delivered using an antegrade transapical approach. The valves were crimped and loaded onto a custom-made inducing system (OD = 8 mm) consisting of a rigid tube and a pusher. The right ventricle was punctured using needle through purse-string sutures. Thereafter, the introducer system was inserted and the valves were delivered into the pulmonary position under guidance of fluoroscopy (BV, Pulsera, Philips, Medical Systems, The Netherlands) and 2D-transoesophageal echocardiography (TEE, Philips, Medical Systems, The Netherlands). The radial expansion of the nitinol stent forced the native pulmonary valve leaflets against the pulmonary artery wall and kept them fixed. The appropriate position and functionality of the implanted valves was confirmed by angiography. In addition, the in vivo functionality was monitored using transoesophageal, transthoracic and/or epicardial echocardiography during the procedure, immediately after implantation, weekly up to 8 weeks, and prior to sacrifice of the animals (by potassium euthanization and exsanguinations under anaesthesia). The pulmonary artery pressure was measured in order to exclude stent-associated stenosis of the pulmonary outflow tract. Anticoagulation (aspirin and warfarin) was maintained until the animals were sacrificed. After 4 weeks ($n = 3$ dTEHVs) and 8 weeks ($n = 3$ dTEHVs; $n = 1$ dHNHV) valves were explanted for further analysis. All animals received humane care and the study was approved by the institutional review boards (Department of Surgery Research Committee: Approval Ref. 2009/096, Animal Research Ethics Committee; Approval Ref. 009/035, Faculty of Health Sciences, University of Cape Town) and in compliance with the guide for the care and use of laboratory animals published by the National Institutes of Health. The transport of explanted tissue for histological analysis was in accordance with the *Convention on International Trade in Endangered Species* (CITES) regulations for transport.

2.7. Qualitative tissue analysis

Representative samples of the explants ($n = 6$ dTEHVs; $n = 1$ dHNHV) and the non-implanted control valves ($n = 2$ dTEHVs; $n = 1$ dHNHV) were analyzed qualitatively for tissue composition using immunohistochemistry and/or histology and compared with native primate (aortic) heart valves from the same animals ($n = 7$). The tissue sections were studied using H&E staining, Masson–Trichrome staining, and Elastic-van-Gieson (eVG) staining. In addition, immunohistochemistry was performed following antigen retrieval using the Ventana Benchmark automated staining system (Ventana Medical Systems, Tuscon, AZ, USA) and antibodies for alpha smooth muscle actin (α-SMA; Clone 1A4; Sigma Chemical Inc.) and CD31 (Clone JC-70A, Dako Inc.). For immunofluoresence staining a primary antibody for MAC-387 (ab22506; Abcam plc, UK) was used (for detailed protocol see Section 2.3). Analysis of the stained sections and cells was carried out using an inverted fluorescence microscope equipped with a CCD camera (ZEISS Axiovert 40 CFL and ZEISS Axioplan II; Carl Zeiss AG). Image processing was performed using the ZEISS AxioVision™ software (Carl Zeiss AG) and the Office Picture Manager software (Microsoft Inc.). For analysis by scanning electron microscopy (SEM), representative samples of the explants ($n = 6$ dTEHVs; $n = 1$ dHNHV) and non-implanted control valves ($n = 2$ dTEHVs; $n = 1$ dHNHV) and native primate heart valves ($n = 7$) of the same animals were fixed using 2% glutaraldehyde and stored in PBS. After preparation, samples were sputtered with gold and investigated with a ZEISS Supra VP Microscope (Carl Zeiss AG).

2.8. Biochemical tissue analysis

Representative samples of the explants ($n = 6$ dTEHVs; $n = 1$ dHNHV; conduit wall including leaflet hinge area), the non-implanted control valves ($n = 2$ dTEHVs; $n = 1$ dHNHV) and native primate heart valves of the same animals ($n = 7$) were lyophilized and analyzed quantitatively by biochemical assays for total DNA, hydroxyproline (HYP) as well as glycosaminoglycan (GAG) content. For measuring the DNA amount, the Hoechst dye method [22] was used with a standard curve prepared from calf thymus DNA (Sigma Chemical Co.). The GAG content was determined using a modified version of the protocol described by Farndale et al., as previously described [23], and a standard curve prepared from chondroitin sulfate from shark cartilage (Sigma Chemical Co.). Hydroxyproline was determined with a modified version of the protocol provided by Huszar et al. [24].

2.9. Grating interferometry

To determine the degradation of the synthetic scaffold material, representative samples of explanted ($n = 1$) and non-implanted ($n = 1$) dTEHVs as well as dHNHVs ($n = 1$; negative control) were evaluated using grating interferometry (GI) and compared to a piece of PGA-P4HB starter matrix ($n = 1$). GI represents an X-ray imaging method that exploits phase information in addition to absorption contrast. The experiments were performed at the TOmographic Microscopy and Coherent rAdiology experimenTs (TOMCAT) beamline of the Swiss Light Source (Paul Scherrer Institute, SLS, Villigen, Switzerland; [25,26]). A photon energy of 25 keV was selected by a double multilayer. The experimental setup consisted of a phase grating downstream of the sample that provides a rectangular-shaped interference pattern at the Lohmann distance (here: 121 mm) [27,28]. At the position of the interference pattern an absorption grating is used to analyze local lateral offset of the pattern, which are proportional to the first derivative of the phase shift caused by the sample. This is done by laterally scanning one grating with several steps over a fraction of the pitch of the absorption grating and then analyzing the pixel-wise intensity distributions by a Fourier-based approach [29].

The samples were embedded in 2% agarose gel within an Eppendorf cylinder for mechanical fixation. The tomography scan was performed with 1601 projections over 180° and 8 phase steps over 2 periods. The total scanning time was approximately 1.5 h. Multi-slice information was combined in three-dimensional images and different stages of the dTEHV constructs were compared with the native/scaffold control materials.

Histogram-based segmentation was applied to the 3D data sets of explanted dTEHV samples in order to determine the volume ratios of biological matrix, PGA and PH4B, respectively if applicable. Structure sizes of PGA threads in the control scaffold were above but so close to the resolution that taking partial volume effects was necessary during segmentation. Thus, a stepwise segmentation process was applied. First, the PGA matrix was determined with thresholding and confirmation by visual inspection. Second, segmented voxels were dilated in order to account for the effect of finite resolution (2 voxels). Third, the combined structures of PGA and PH4B were segmented and confirmed by visual inspection. Fourth, the substraction of the individual PGA and the combination of PGA and PH4B yielded the PH4B part of the sample. Finally, scaffold volume was estimated by manually drawing a smooth bounding box around the outer visible threads. This procedure was applied to 6 representative slices.

2.10. Statistics

The measurements of the transvalvular peak pressure gradient, international normalized ratio, and grade of regurgition are provided as mean ± standard deviation (SD). Biochemical measurements are presented as mean ± standard error of the mean (SEM). One-way ANOVA was used to determine the differences between the dTEHVs explanted after 4 weeks, 8 weeks, and native valves with respect to DNA and extracellular matrix contents (control groups and the dHNHV explant were neglected for statistical analyses given the low case number, $n < 3$). STATGRAPHICS software (Statistical Graphics corp., USA) was used for statistical analysis with $p < 0.05$ considered as statistically significant.

3. Results

3.1. Morphology and phenotype of human fibroblasts

Outgrowing human vascular-derived fibroblasts displayed a typical spindle-shaped pattern (Fig. 1a) and expressed high levels of vimentin (Fig. 1b). Expression of α-smooth muscle actin, desmin, and CD45 was not detected (Fig. 1c–e). This morphology and staining pattern is characteristic for fibroblastic cells and comparable to the common phenotype of cells isolated from human cardiovascular tissues.

3.2. Macroscopic appearance of implanted valves

Macroscopically the decellularized tissue-engineered heart valves (dTEHVs) revealed thin, shiny tissue formation in the wall and the leaflets, with no visible changes upon decellularization (Fig. 2A). However, after separation of the leaflets of the dTEHVs,

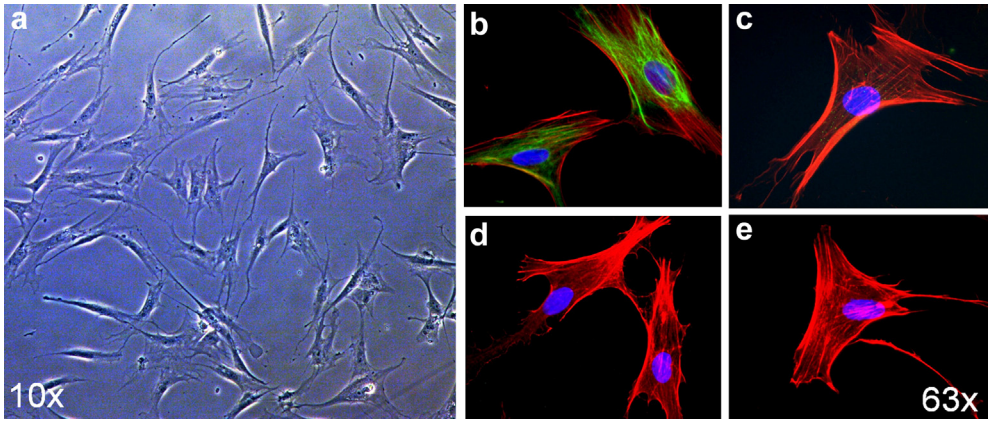

Fig. 1. Human vascular-derived fibroblasts. The isolated and expanded cells presented a typical spindle-shaped pattern (a) with expression of vimentin (b), but no expression of α-SMA (c), desmin (d), or CD45 (e).

just before implantation, reduced coaptation of the leaflets was observed (see Fig. 2B). The decellularized human native heart valve (dHNHV) controls, incorporated into nitinol stents (Fig. 2C) similar to the dTEHVs, revealed no visible changes following the process of decellularization.

3.3. Microscopic analysis of the control implants

Analysis of the scanning electron microscopy (SEM) samples of the dTEHVs (Fig. 3a–g) revealed layered tissue composition in the transversal plane (Fig. 3a–d) suggesting layered collagen arrangement within the leaflet and wall interstitium. Moreover, no cellular structures or remnants could be identified, neither in the dTEHV samples (Fig. 3b–g) nor in the dHNHV leaflets (Fig. 3h–j). These findings were confirmed by histological analyses. In eVG stainings, of both the dTEHVs and the dHNHV (Fig. 4) layered collagen arrangement was observed and also the absence of cells in the leaflets and wall of the dTEHVs (Fig. 4a–d) was demonstrated by histology. The leaflets of the dHNHV showed almost complete decellularization (Fig. 4e–h) as single cellular remnants were present in eVG staining. Also in the border zone of the wall structures some cellular remnants could be identified (Fig. 4g–h). While elastin could not be detected in the dTEHV (Fig. 4a–d) constructs, eVG staining of the dHNHV showed collagen and elastin arrangement in the leaflets and wall regions, as is typical for native heart valves (Fig. 4e–h).

3.4. Implantation and in vivo performance of the valves

For evaluation of the in vivo functionality and host repopulation in non-human primates, dTEHVs and dHNHV were successfully implanted into the orthotopic pulmonary valve position using a transapical approach (Fig. 5a,b). The mean crimping time of the dTEHVs was 7.3 ± 2.4 min from insertion into the application system until surgical deployment. The crimping time for the dHNHV control was 5.7 min. No early or late mortality occurred in the study animals and all valves were followed up until the projected harvesting time point. Positioning of the valves was verified intra-operatively using TEE and fluoroscopy (Fig. 5c–f). Neither migration of the implanted valves nor paravalvular leakage was detected during the follow-up period. After deployment valvular functionality with leaflet mobility and sufficient opening was demonstrated using TEE measurements. However, immediately after deployment of the valve mild to moderate central valvular regurgitation was observed for the dTEHVs, which persisted over the entire study period and slightly increased in the last weeks of the long term (8 week) follow-up group (Table 1). Weekly TTE/TEE follow-up revealed an increased transvalvular peak pressure gradient compared to perioperative measurements (TVG; Table 1). After 4 weeks the dTEHVs showed still mobile and pliable cusp-like leaflet structures by echocardiography (Fig. 6a–d), however no full coaptation was observed as the leaflets were shortened in the radial direction. Similar echocardiographic results (Fig. 6g–j) were obtained after 8 weeks follow-up of the dTEHVs.

In three of the implanted dTEHVs local dehiscence of the valvular conduit was noted during follow-up echocardiography, which could be verified at the time of explantation. The dHNHV control showed sufficient in vivo functionality with flexible leaflets, good coaptation, and proper opening and closing behavior during follow-up time up to 8 weeks (Fig. 6m–p). Although mild regurgitation was present immediately after implantation, no significant regurgitation was detected after 8 weeks.

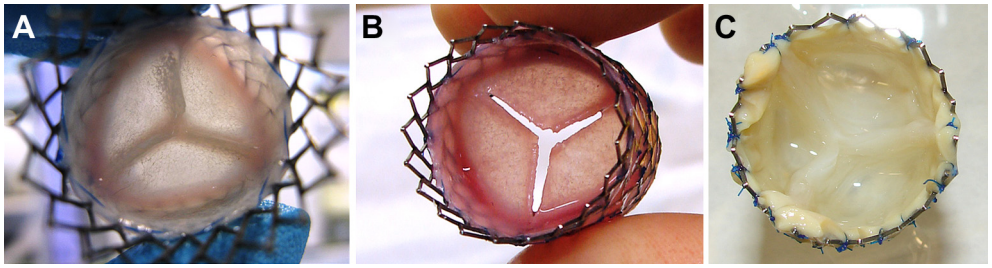

Fig. 2. Macroscopic appearance of the implants. Decellularized tissue-engineered heart valves (dTEHVs) revealed thin, shinny tissue in wall and leaflets (A). However, reduced coaptation of the leaflets (B) was observed after separation of the fused leaflets of the dTEHV, just before implantation. The decellularized human native heart valve (dHNHV) control was incorporated in nitinol stents (C) similar to the dTEHVs to serve as a control during in-vivo follow-up.

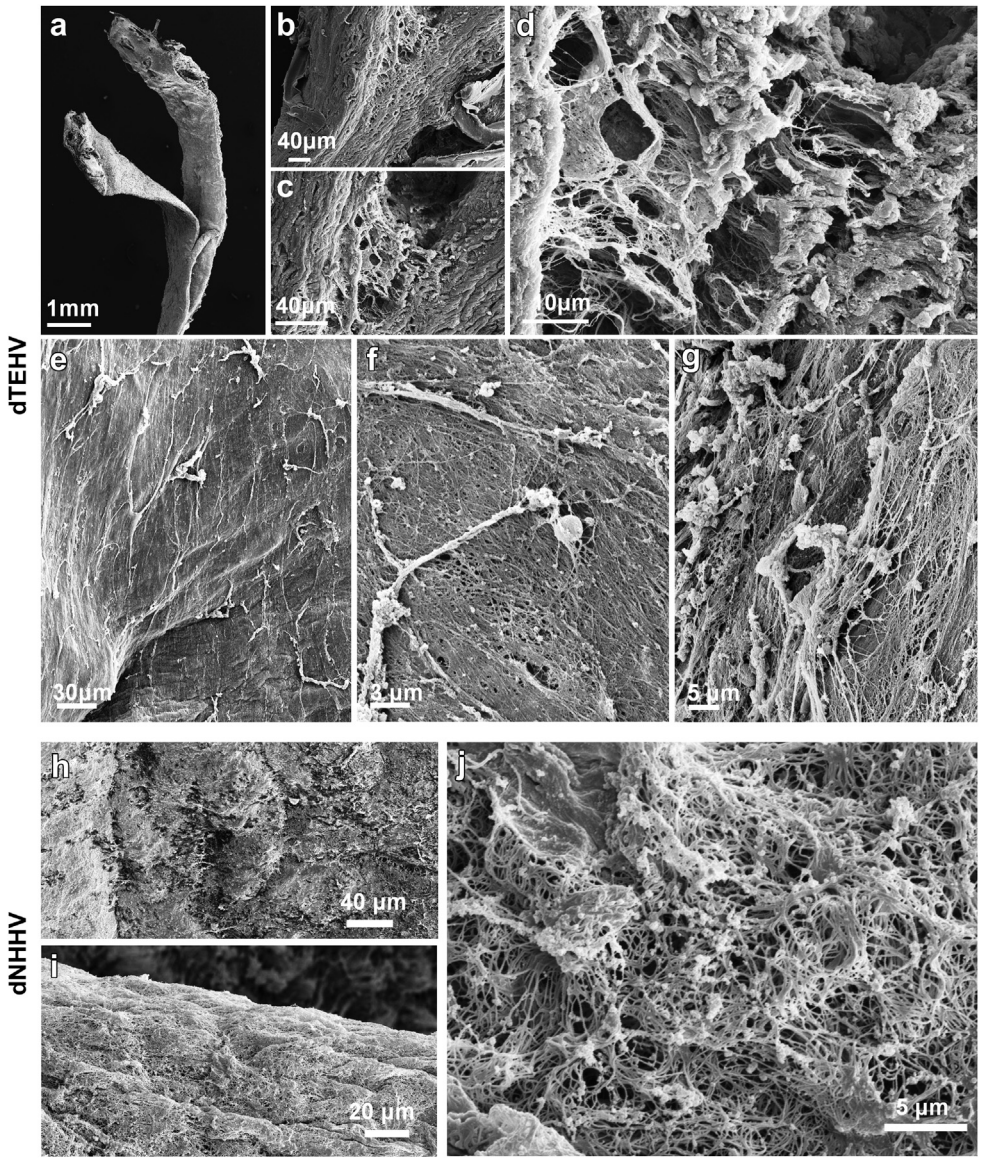

Fig. 3. SEM analysis of the control implants. Scanning electron microscopy (SEM) analysis of decellularized tissue-engineered heart valves (dTEHVs, a–g). The transversal cut (with increasing magnification from a to d) revealed layered arrangement of collagen fibers (b–d). The absence of cells on the surface of the leaflets (e–g) demonstrated complete decellularization with remaining extracellular matrix components. SEM analysis of a decellularized human native heart valve (dHNHV, with increasing magnification from H to J) also demonstrated complete decellularization of the leaflet surfaces.

3.5. Macroscopic appearance of the explanted valves

Explantation of the dTEHVs ($n = 3$) after 4 weeks follow-up revealed bioengineered tissues that were well integrated into the adjacent cardiac tissue. Tissue covering the proximal stent margin and encircling stent strut endings suggested trans-anastomotic integration of the bioengineered tissues into the surrounding cardiac environment. The 4 week explants exhibited white, shiny tissue surfaces without sign of thrombotic depositions. The thin and pliable, mobile cusps (Fig. 6e–f) revealed a small further reduction in the radial direction when compared to the leaflet size at implantation (Fig. 2a–b), which explained the lack of coaptation observed by echocardiography (Fig. 6a–d). Macroscopic analysis of the explanted dTEHV after 8 week follow-up again presented with pliable, mobile cusps (Fig. 6k–l) with no evidence of thickening or thrombus formation. In one of the 8-week explants a thickening of the conduit was observed at the ventricular side. Also the radial size of the leaflets in the 8 week explants was, similar to the 4 weeks explants, reduced when compared to the implants (Fig. 6k). No macroscopic evidence of thickening or thrombus formation was observed in the explanted dHNHV (Fig. 6q–r). Moreover, ex-vivo leaflet geometry was similar to the implanted geometry and therefore comparable to clinically used xeno- or allogenic transplants.

3.6. Matrix morphology and cellularity of the explanted valves

Microscopically, all explanted tissues demonstrated layered tissue morphology (Fig. 7) with comparable leaflet thickness. The explanted dTEHVs revealed remnants of scaffold material in the central core of the leaflets (Fig. 7c–e; arrows) and – although already more resorbed – in parts of the wall (Fig. 7d–f). Masson's Trichrome and Elastic van Gieson (eVG) staining showed the presence of collagen throughout all explanted leaflet and wall structures (Fig. 7; 2nd and 4th column).

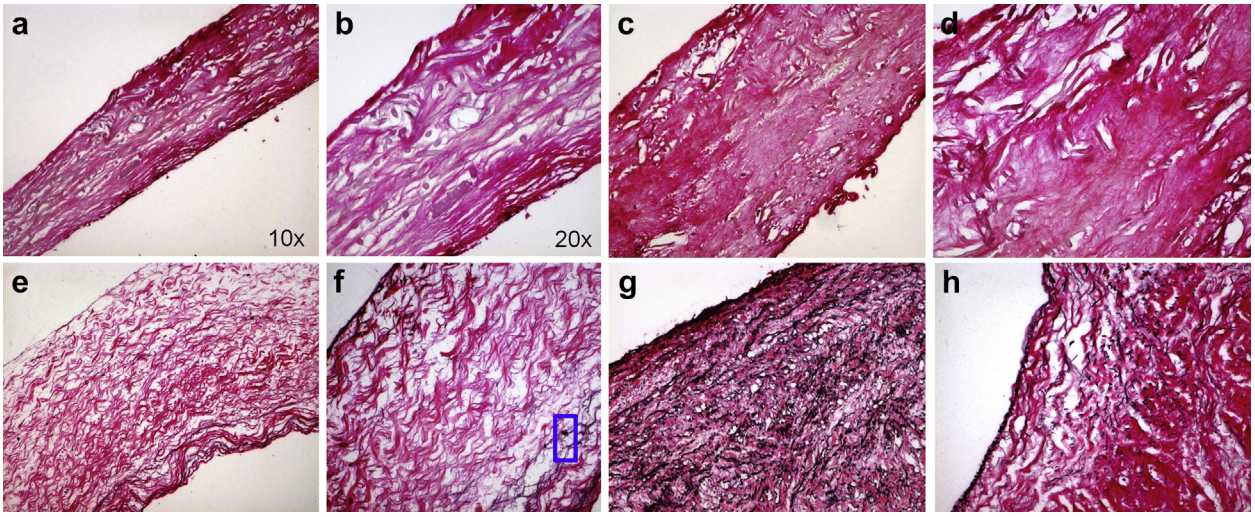

Fig. 4. Histological analysis of the control implants. Elastic van Gieson (eVG) staining (a–h) of decellularized tissue-engineered heart valves (dTEHVs; a–d) and decellularized human native heart valves (dHNHVs; e–h) of both leaflets (a,b,e,f) and wall (c,d,g,h). Layered tissue formation and collagen arrangement was observed in all tissues, with only remnants of scaffold in the center of the dTEHVs (a–d; mainly P4HB remnants). Although elastin was not detected in the dTEHV (a–d), eVG staining of dHNHVs showed collagen and elastin arrangement in the leaflets and wall regions, as is typical for native heart valves (e–h). Complete decellularization is demonstrated for the leaflets and wall of the dTEHVs (a–d) and almost complete decellularization of the dHNHVs leaflets (e–f; blue square indicates a remnant nucleus). Also in the border zone of the wall of the dHNHV control cellular remnants could be identified (g–h). (For interpretation of the references to color in this figure legend, the reader is referred to the web version of this article.)

Remarkably, all explanted dTEHVs presented substantial, homogeneous cellular repopulation, as visualized by hematoxylin–eosin staining (Fig. 7c–f). Moreover, the cellularity of the leaflets (Fig. 7c,e) was comparable to that of native leaflets (Fig. 7a). In the conduit the repopulation was even more pronounced (Fig. 7d) and was even further increased in the 8 week explanted dTEHVs (Fig. 7f).

Immunohistochemical analysis revealed α-SMA positive elements in the conduit wall of all valves (Fig. 7r,t,v). Remarkably, the repopulated dTEHV leaflets showed no expression of α-SMA (Fig. 7s,u), comparable to native leaflet structures (Fig. 7q). However, the leaflet and wall structures of 4 and 8 week explants showed surface-mediated cells that stained positive for MAC-387 suggesting macrophage infiltration of the dTEHV constructs (Suppl. Fig. 1a–b). In contrast to the native leaflet and wall structures, no elastin could be detected by eVG stainings of the 4 and 8 week explanted dTEHVs (α-δ).

In contrast to the rapidly repopulated dTEHVs, the dHNHV leaflets and conduit structures showed only surface-mediated cell repopulation 8 weeks after implantation. No cells were found in the leaflet interstitium (Fig. 7g), while in the conduit part (Fig. 7h) cells were sparsely present in the region of the anterior (luminal) and

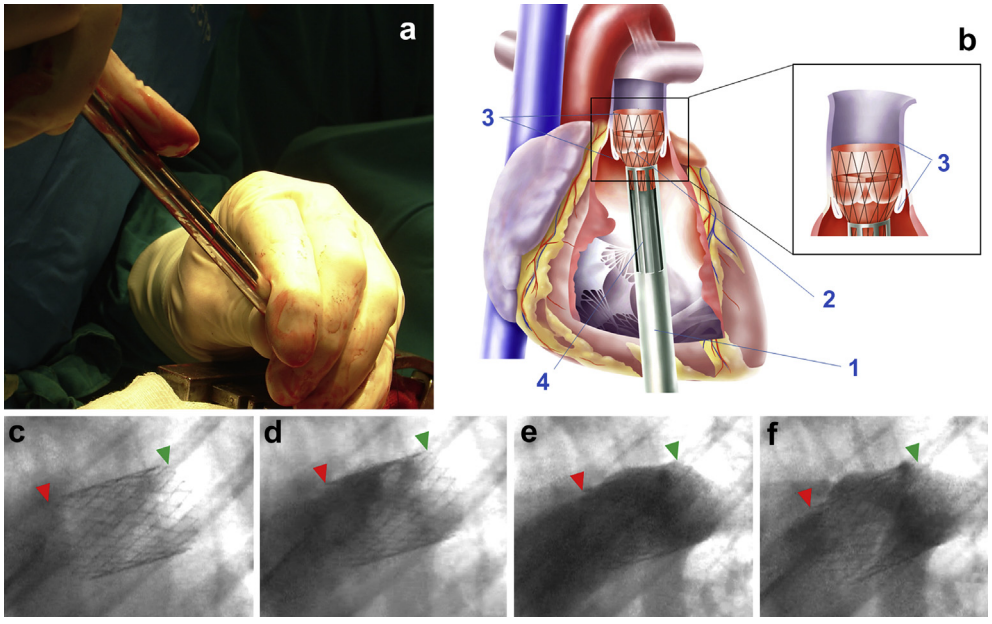

Fig. 5. Minimally invasive transapical heart valve implantation. For interventional delivery (a) the stented valves were loaded into the delivery device (b1), whereafter the device was inserted into the right ventricle and the stented valves (b2) were deployed into the pulmonary position (b3) under sonographic and fluoroscopic guidance (c–f). The crimped valve (b2) integrated into the nitinol stent is carefully deployed at the pulmonary position (b3) by slowly advancing the inner pusher into the sheath system (b4).

Table 1
Measurements (mean ± SD) of transvalvular peak pressure gradient (TVG in mmHg), international normalized ratio (INR), and grade of regurgitation during 8 weeks follow-up of orthotopically implanted decellularized tissue-engineered heart valves (dTEHVs).

Value	Implant	1 week	2 weeks	3 weeks	4 weeks	7 weeks	8 weeks
TVG[a]	2.56 ± 0.97	8.98 ± 5.54	17.13 ± 5.65	11.66 ± 5.19	13.57 ± 3.08	19.8 ± 7.16	12.8 ± 4.41
INR[b]	–	1.05 ± 0.05	1.37 ± 0.34	1.25 ± 0.29	–	1.07 ± 0.12	[d]
Regurgitation[c]	2.83 ± 0.26	2.67 ± 0.60	2.75 ± 0.42	3.08 ± 0.2	2.75 ± 0.29	2.83 ± 0.29	3.33 ± 0.29

[a] TVG = Transvalvular Peak Pressure Gradient.
[b] INR = International Normalized Ratio.
[c] Regurgitation – Grading: 0/1/2/3/4 – None/trivial/mild/moderate/severe.
[d] Explantation.

posterior (ante-luminal) border zones. While the cells on the leaflet surfaces and vascular conduit surfaces may predominantly represent endothelial cells (see Section 3.7), the posterior cell population represents either cellular remnants of the decellularization procedure (as also observed in the non-implanted controls) or first signs of a trans-anastomotic repopulation.

3.7. Endothelialization of the valves

While only sparse endothelialization was observed for the leaflets of the explanted dTEHVs after 4 and 8 weeks in vivo (Fig. 7), most areas of the surface of the conduit wall were densely covered by a confluent endothelial layer as shown with SEM (see Fig. 8a–g). The cellular phenotype and arrangement of this endothelial coverage was comparable to those of native primate heart valve leaflets. However, in some regions of dTEHV leaflets, for both 4 and 8 week explants, a more premature surface remodeling was detected (Fig. 8g), characterized by areas with extensive fibrin deposition as well as leukocyte and thrombocyte attachment, with beginning provisional thrombocyte-mediated surface coverage. Interestingly, these regions were located in close proximity to areas of almost confluent endothelial covering.

3.8. Repopulation and extracellular matrix remodeling

Quantitative measurements of the hydroxyproline values of the dTEHV explants, representative for the amount of collagen, revealed comparable collagen amounts in all groups, which were in the range of that of native primate heart valves (Fig. 9A). The glycosaminoglycan content of the dTEHV was significantly increased after 8 weeks in vivo (Fig. 9B) when compared to values of native primate heart valves, suggesting in situ formation of glycosaminoglycans. The glycosaminoglycan level of the non-implanted dHNHV was low compared to the native primate valves and did not increase after 8 weeks in vivo (Fig. 9B). Cell removal of the non-implanted dTEHVs was confirmed as DNA was non-detectable in these control valves (Fig. 9C). Although the decellularization of the non-implanted dHNHV control was not complete prior to implantation (Fig. 9C), the explanted dHNHV presented non-detectable levels of DNA, which quantitatively confirms the lack of host cell repopulation 8 weeks after implantation (Fig. 9C). In contrast, the amount of DNA of dTEHV explants after 4 weeks in vivo (Fig. 9C) was comparable to the native heart valves and significantly increased after 4 additional weeks in vivo, confirming histological observations.

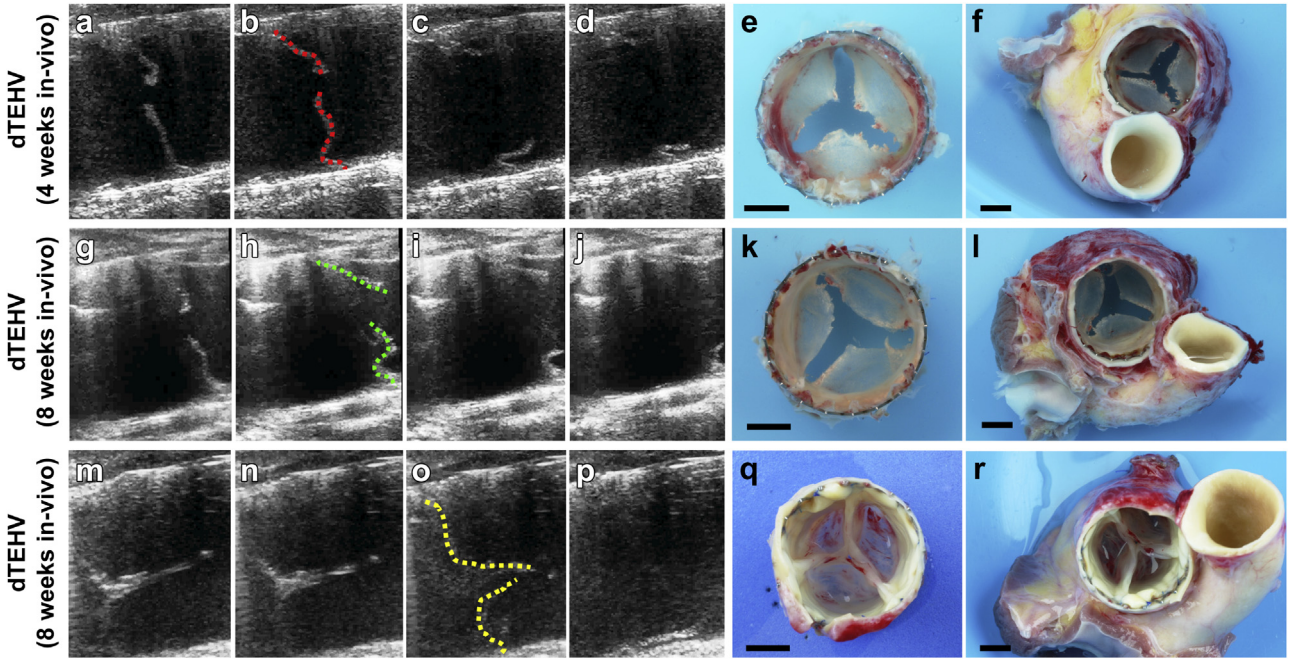

Fig. 6. Functionality and macroscopic outcome of the valves. Decellularized tissue-engineered heart valves (dTEHVs) showed mobile and pliable cusp-like leaflet structures by echocardiography 4 weeks after implantation (a–d). As the leaflets were shortened in the radial direction (a, and indicated by the red lines in b) coaptation was lacking. The 4 week explants (e–f) confirmed the reduced leaflet size, but leaflet tissue was thin, shiny and without signs of thrombotic depositions. After 8 weeks follow-up, the dTEHVs demonstrated similar echocardiographic (g–j) and macroscopic results (k–l) without further reduction of the leaflet size. The dHNHV showed in-vivo functionality and ex-vivo leaflet geometry comparable to clinically used xeno- or allogenic transplants (m–r). (For interpretation of the references to color in this figure legend, the reader is referred to the web version of this article.)

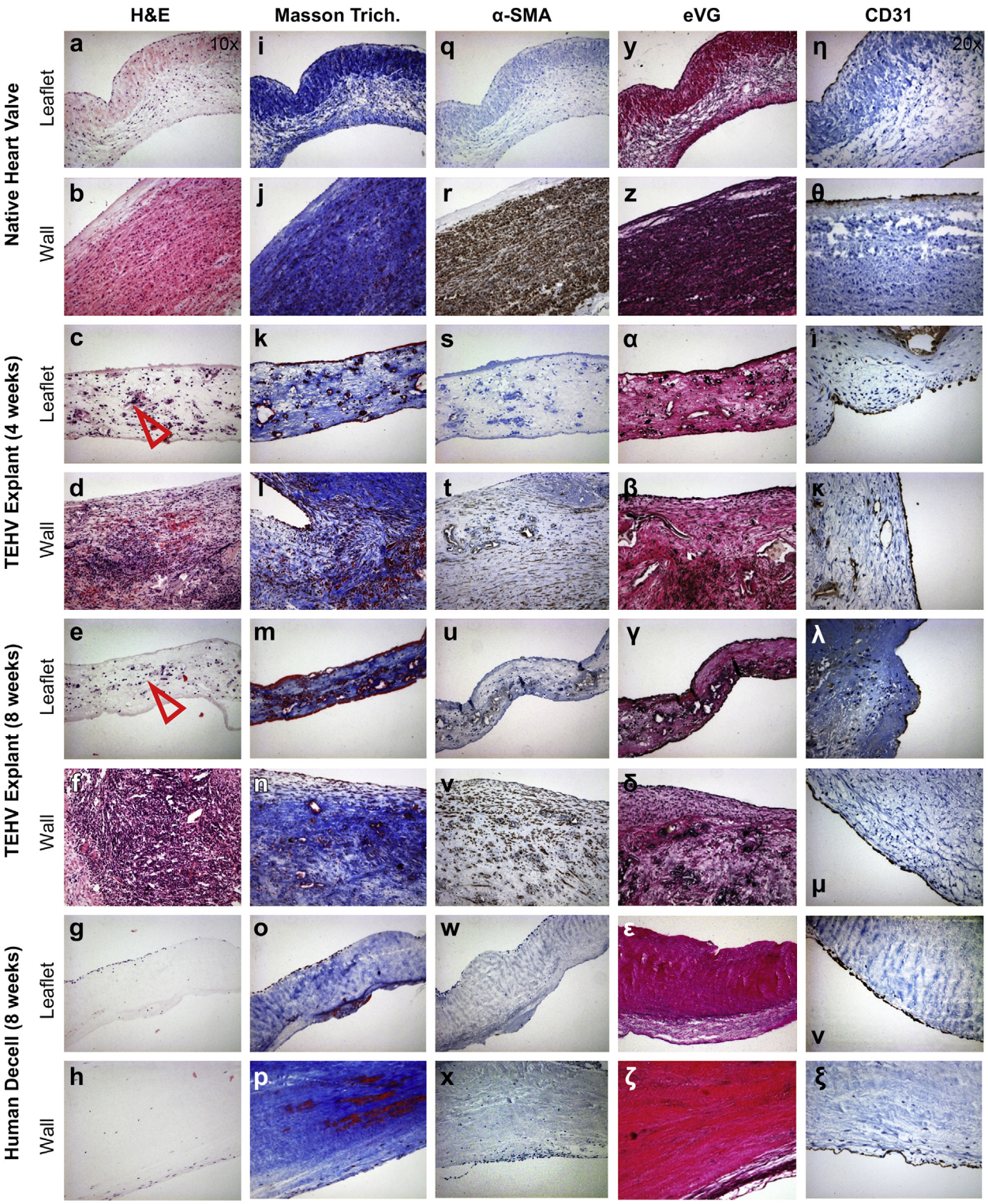

Fig. 7. Histology and immunohistochemistry of the explanted valves. Representative samples of decellularized tissue-engineered heart valves (dTEHVs) explanted after 4 weeks (3rd and 4th row) and 8 weeks (5th and 6th row) compared to the explanted decellularized human native heart valve (dHNHV) after 8 weeks (7th and 8th row) and primate native heart valve (1st and 2nd row). All tissues showed layered tissue architecture in H&E staining with only minor scaffold components in the explanted dTEHVs (c–f). The cellularity of the leaflets visualized by hematoxylin–eosin staining (H&E) in the explanted dTEHVs (c,e) was comparable to that of native leaflets (a), while the wall cellularity of the 4 weeks explants (d) was further increased in the 8 week explanted dTEHVs (f). The dHNHV leaflets showed no cellularization of the interstitium, only on the surface recellularization was present (g). Also in the wall mainly surface-mediated recellularization was observed (h). Masson Trichrome staining (second column) and Elastic van Gieson (eVG, fourth column) revealed the presence of collagen bundles in all explanted leaflet and wall structures (i–p). Immunohistochemical analysis revealed no expression of α-SMA in any of the explanted leaflets (s, u, w) just like in the native leaflets (q). Moreover, in the wall of all explants and native valves α-SMA positive cells could be identified (r,t,v), although remarkably less in the explanted dHNHV (x). No elastin was detected by eVG stainings of the 4 and 8 week explanted dTEHVs (α-δ) while dHNHV (ζ) as well as primate native valves (z) showed presence of elastin elements. Analysis of CD31 expression showed endothelialization of all explants and control constructs. However, the dTEHV leaflets (4 and 8 week explants) showed only partial endothelialization (ι, λ), while the wall regions showed confluent endothelial linings (κ, μ). Images were taken at 20× magnification.

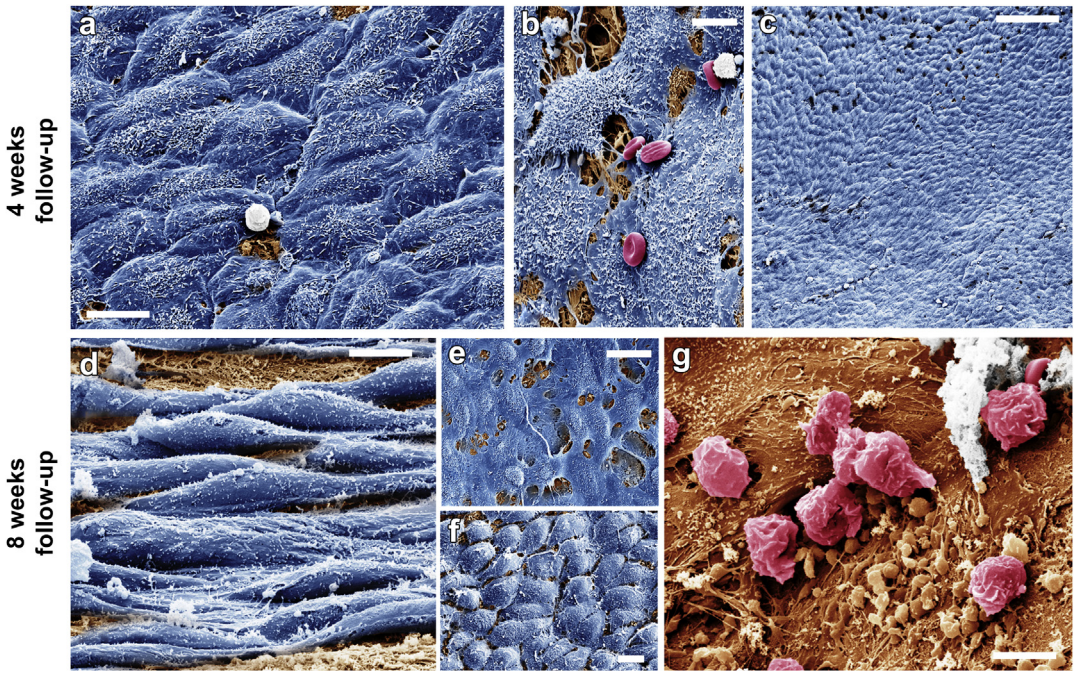

Fig. 8. Endothelialization of the explanted valves. Scanning electron microscopy (SEM) showed both partially endothelialized areas (a–b, 4 week explants; d–f 8 week explants) and confluent areas with morphological appearance comparable to native at all explantation time points (c). However, in some regions of the dTEHV explants, for both 4 and 8 weeks explants, no endothelial cells were present and exhibited extensive fibrin deposition as well as leukocyte and thrombocyte attachment, with beginning provisional thrombocyte-mediated surface coverage (g). Interestingly, these regions of more premature surface remodeling were located in close proximity to areas of almost confluent endothelial covering.

3.9. Grating interferometry

For assessment of the presence of scaffold remnants in the explanted dTEHV constructs grating interferometry (GI) based segmentation analysis of representative samples was performed (Fig. 10; total: $n = 4$; $n = 1$ per group). Segmentation GI analysis revealed a total volume component of the PGA scaffold portion of 8 ± 4% and a P4HB component of 0.9 ± 0.3% (Fig. 10a–b). For the non-implanted dTEHV control construct small thread-like structures with sizes close to the resolution (15 microns) were observed, which represents most likely residues of the degraded PGA component and suggest almost full deterioration of the PGA. However, the resolution was insufficient for a reliable segmentation of the PGA in this construct. Therefore, only the ratio between PH4B and biological matrix was determined for the entire 3D data set, which was confirmed by visual inspection revealing a portion of 4.0 ± 1.0% for the P4HB (Fig. 10c–d). For explanted tissue (8 week follow-up) contrast and resolution was sufficient in the entire 3D data set to segment P4HB filaments by thresholding, where the threshold was determined by a standard maximum entropy approach revealing a comparable amount of P4HB per total volume (4.8 ± 0.6%; Fig. 10e–f). Although limited by the small sample size, these results suggest that PGA undergoes almost complete degradation already prior to in vivo implantation throughout the dynamic conditioning and decellularization procedure, while the P4HB component remains present over longer in vivo periods (without detectable degradation).

4. Discussion

Given the substantial risk for thromboembolic complications and the associated need for lifelong anticoagulation therapy in mechanical heart valve prostheses, xenogenic or – if available – allogenic materials represent a valuable alternative for heart valve replacement therapy in particular in children and young adults [8]. Although such replacements are lifesaving, these fixed or cryopreserved materials are highly prone to calcification, degeneration and failure [3–6] – a process that is even accelerated in young patients due to their high immunological competence [30].

This substantial shortcoming of the currently available replacement materials has stimulated the concept of cardiovascular tissue engineering aiming at the fabrication of non-immunogenic, autologous cell-based constructs with regeneration and remodeling potential. These living autologous constructs were based on fully biodegradable synthetic (bio)materials, which have proven growth-adaptive behavior in several preclinical investigations [31,32]. In spite of the experimental success of the heart valve tissue engineering technology, the substantial technological and logistical complexity – also involving regulatory approval of ex-vivo cell processing procedures – has so far slowed down the routine clinical translation of autologous living cardiovascular tissue-engineered constructs [18]. Being a less complex alternative, decellularized xenogenic or allogenic heart valves have been investigated as starter matrices for “tissue engineering” of valve replacements with promising experimental as well as first clinical results [7,8]. However, xenogenic materials are associated with the risk of immunogenic reactions as well as zoonotic disease transmission and the availability of healthy human, allogenic materials is naturally highly limited [11]. Therefore, decellularized TEHVs based on biodegradable synthetic materials and homologous cells have recently been developed as potential “off-the-shelf” homologous alternatives [19] and are currently under investigation in preclinical trials in the ovine model. Importantly, these substitutes would combine several advantages of different

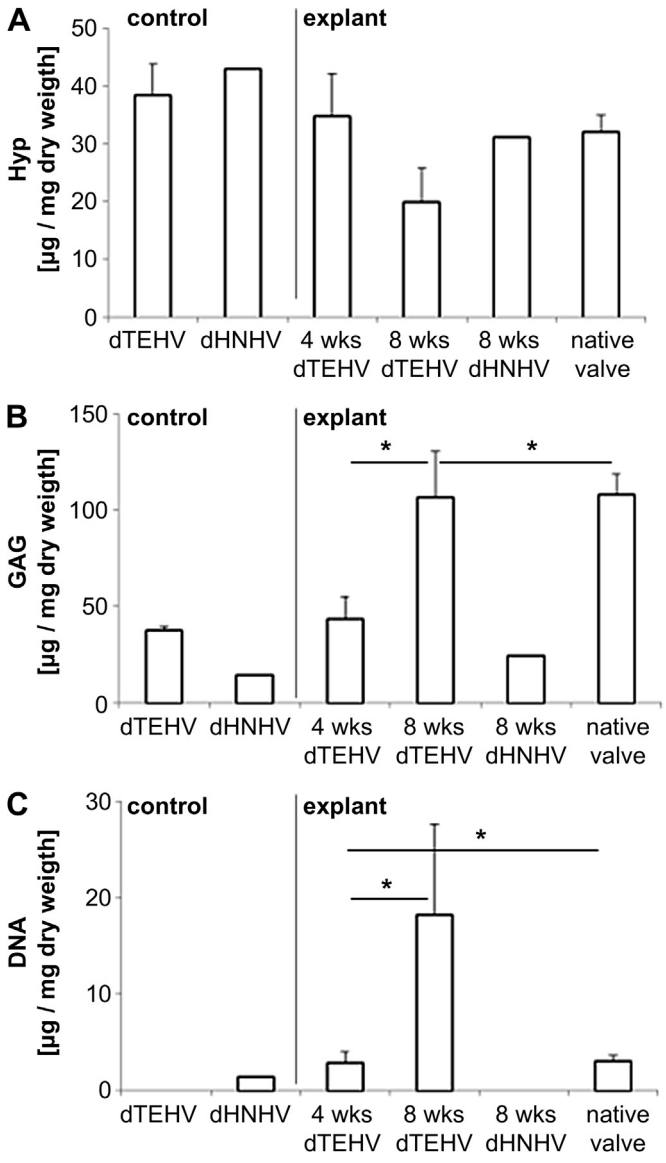

Fig. 9. Quantitative DNA and extracellular matrix analysis. Quantitative measurements of amounts of hydroxyproline (HYP, A), glycosaminoglycan (GAG, B), and DNA (C). The amount of HYP was comparable for all groups. Compared to the levels of the explant dTEHVs after 4 weeks, the GAG levels B were significantly increased after 8 weeks in vivo to approximate the values of native primate heart valves. The GAG level of the non-implanted dHNHV was low compared to the values of native primate valves and did not significantly change in vivo. Cell removal of the non-implanted dTEHVs was confirmed as amounts of DNA were non-detectable. Also low amounts of DNA were measured for the non-implanted dHNHV and the explanted dHNHV. The cellularity of dTEHV explants after 4 weeks in vivo was comparable the native heart valves and significantly increased after an additionally 4 weeks in vivo. (*$p < 0.05$).

technologies in one construct: human cell-derived matrices for guided tissue regeneration and host cell repopulation with regeneration and growth capacities as well as decellularized homologous (non-xenogenic) 'off-the-shelf' replacement structures available in unlimited numbers. After proving the in vitro feasibility [19] and initiating preclinical investigations in the ovine model, the present study focused on the in vivo assessment of human fibroblast-derived decellularized tissue-engineered heart valves (dTEHVs) in a non human-primate model representing a model with cellular in situ remodeling characteristics close to the human cardiovascular environment.

In recent studies we have already demonstrated the principal feasibility of merging autologous cell-based heart valve tissue engineering procedures and minimally invasive implantation techniques in the ovine and non-human primate model. However – although the sheep model is still considered as the relevant model for preclinical regulatory approval (worst case calcification model) – these investigations revealed that the findings in the ovine model cannot be transferred directly to the non-human primate level [17], which is of major relevance when considering the clinical translation of the cardiovascular tissue engineering concept. Interestingly, the phenomenon of leaflet thickening, which was observed in the ovine model already 4 weeks after implantation [16], was not observed to the same extend in non-human primates [17]. Also in the present investigation no thickening of the leaflet structures – neither in the dTEHV nor in the dHNHV control leaflets – was observed. However, as observed by previous studies in vitro [33,34] and in vivo (in the ovine [16] as well as in the primate model [17]), a shortening of the leaflets was evident in the dTEHVs in the present investigation (but not in the dHNHV control leaflets). Moreover, in the current study (functional) leaflet shortening (minimizing valvular coaptation) was already present after leaflet separation prior to delivery, which was most likely due to the flat dTEHV leaflet position (acute leaflet opening angle). This flat valve geometry due to the in-vitro production process resulted in insufficient valvular coaptation in vivo and explains the mild-moderate regurgitation present in the valves right after delivery. Given this suboptimal valve geometry (and the associated suboptimal load distribution), the functionality of the leaflets was remarkable and remained stable up to 8 weeks after implantation with high mobility of the leaflets.

In addition, the dTEHVs presented with fast (4 weeks), increasing and homogenous cellular repopulation in the leaflet as well as the wall structures, while the dHNHV control leaflets showed only minimal surface-mediated recellularization, that may even have resulted from the incomplete decellularization procedure in this valve. This suggests that in the acute phase of remodeling dTEHVs allow for faster and higher recellularization and may represent ideal 'frameworks' for host cell repopulation and remodeling. Interestingly, the increase of cellularization from 4 to 8 weeks was most evident in the conduit area of the explants. A further enhancement of cellular repopulation of the leaflet areas may therefore represent another factor supporting optimal dTEHV in vivo remodeling. Besides the number, the phenotype of the repopulated cells is of fundamental importance for the fate of the tissue-engineered constructs. In previous studies, the constructs generated in vitro as well as their vivo explants [16,17] showed a high fraction of cells with α-smooth muscle actin (α-SMA) positive phenotypes in the leaflet and conduit areas. This (α-SMA-positive) contractile valve interstitial cell phenotype – which is usually only present during valve embryology and/or pathology [35,36] – has been intensively discussed as a potential factor in valvular leaflet shortening and retraction [33,34]. Although decellularization of the TEHV removes the cell-induced retraction of the leaflets [19], residual stresses in the extracellular matrix, build up during culture of the leaflets in closed configuration, still accounts for mild retraction after separation of the leaflets. This passive retraction of the extracellular matrix further reduces the coaptation area of the valve leaflets. Interestingly, in the present investigation no α-SMA-positive elements were found in the dTEHV leaflet structures comparable to the (rather quiescent) native valve interstitial cell compartment suggesting absence of 'active' leaflet shortening originating from the repopulated cells. However, the dTEHV leaflet and wall structures showed presence of MAC-387 positive cells suggesting significant infiltration of macrophages already after 4 weeks in vivo.

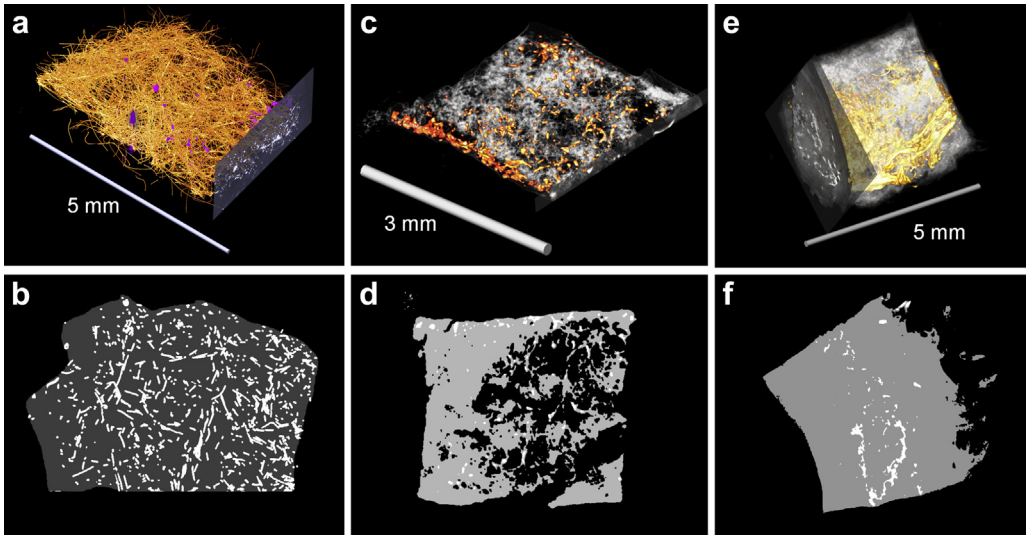

Fig. 10. Grating interferometry-based segmentation analysis. Grating interferometry analysis of the scaffold starter matrix (a–b) shows that both components – the PGA (orange) and the P4HB (violet) – are present. After dynamic conditioning and decellularization the dTEHVs show substantial degradation of the PGA component, while the P4HB component remains without detectable changes (c–d). After 8 weeks in vivo the dTEHV explants show presence of the P4HB component (e–f; a,c,e represent 3D reconstructions; b,d,f represent segmented images). (For interpretation of the references to color in this figure legend, the reader is referred to the web version of this article.)

5. Conclusions

These initial results of combining heart valve in vitro tissue engineering, decellularization protocols and minimally invasive valve replacement procedures are promising and demonstrate the feasibility of using dTEHVs for valve replacement in the non-human primate model. Most importantly, these "off-the-shelf" available homologous (non-xenogenic) valve replacement materials hold the potential to overcome the limitations of current clinically used fixed, decellularized and cryopreserved allogenic and/or xenogenic valve replacement materials. Besides further enhancement of leaflet recellularization, the improvement of the valvular geometry and increasing coaptation areas seems crucial. Beyond this feasibility study, extended long-term studies are mandatory in order to further elucidate the fate of these repopulated human cell-derived dTEHVs in vivo as well as to better understand the underlying tissue remodeling mechanisms involved. Particularly, the phenotype and precise role of the repopulating cells with respect to their function in chemo-attraction and tissue formation have to be systematically assessed.

Conflict of interest

The authors have no conflicts of interest to declare.

Acknowledgments

This study represents a collaborative approach. The authors thank Klaus Marquardt (ZMBZ), Andres Kaech (ZMBZ), Peter Vogt, Pia Fuchs and all members of the research facilities in Zurich, Eindhoven and Cape Town. This work was supported by the Swiss South African Joint Research Programme of the State Secretariat for Education and Research, Swiss and South African Governments [EX25-2010], the Swiss National Science Foundation [32-122273], [310030-143 992] and [124090]; the 7th Framework Programme – Life Valve of the European Commission [242008]; the Research Infrastructure Support Programme [UID 65720]; the National Research Foundation and the Department of Science and Technology South Africa, the University Research Committee – University of Cape Town; the Claude Leon Foundation; the Centre d'Imagerie BioMedicale (CIBM) of the UNIL, UNIGE, HUG, CHUV, EPFL, the Leenaards and the Jeantet Foundations.

Appendix A. Supplementary data

Supplementary data related to this article can be found online at http://dx.doi.org/10.1016/j.biomaterials.2013.04.059.

References

[1] Yacoub MH, Takkenberg JJ. Will heart valve tissue engineering change the world? Nat Clin Pract Cardiovasc Med 2005;2:60–1.
[2] Iung B, Vahanian A. Epidemiology of valvular heart disease in the adult. Nat Rev Cardiol 2011;8:162–72.
[3] Kobayashi J. Stentless aortic valve replacement: an update. Vasc Health Risk Manag 2011;7:345–51.
[4] Mankad S. Management of prosthetic heart valve complications. Curr Treat Options Cardiovasc Med 2012;14:608–21.
[5] Pibarot P, Dumesnil JG. Prosthetic heart valves: selection of the optimal prosthesis and long-term management. Circulation 2009;119:1034–48.
[6] Schoen FJ. Evolving concepts of cardiac valve dynamics: the continuum of development, functional structure, pathobiology, and tissue engineering. Circulation 2008;118:1864–80.
[7] Baraki H, Tudorache I, Braun M, Höffler K, Görler A, Lichtenberg A, et al. Orthotopic replacement of the aortic valve with decellularized allograft in a sheep model. Biomaterials 2009;30:6240–6.
[8] Cebotari S, Tudorache I, Ciubotaru A, Boethig D, Sarikouch S, Goerler A, et al. Use of fresh decellularized allografts for pulmonary valve replacement may reduce the reoperation rate in children and young adults: early report. Circulation 2011;124:S115–23.
[9] Patience C, Takeuchi Y, Weiss RA. Infection of human cells by an endogenous retrovirus of pigs. Nat Med 1997;3:282–6.
[10] Moza AK, Mertsching H, Herden T, Bader A, Haverich A. Heart valves from pigs and the porcine endo-genous retrovirus: experimental and clinical data to assess the probability of porcine endo-genous retrovirus infection in human subjects. J Thorac Cardiovasc Surg 2001;121:697–701.
[11] Llames S, García E, Otero Hernández J, Meana A. Tissue bioengineering and artificial organs. Adv Exp Med Biol 2012;741:314–36.
[12] Weber B, Emmert MY, Schoenauer R, Brokopp C, Baumgartner L, Hoerstrup SP. Tissue engineering on matrix: future of autologous tissue replacement. Semin Immunopathol 2011;33:307–15.
[13] Weber B, Emmert MY, Hoerstrup SP. Stem cells for heart valve regeneration. Swiss Med Wkly 2012;16:142.
[14] Emmert MY, Weber B, Wolint P, Behr L, Sammut S, Frauenfelder T, et al. Stem cell-based transcatheter aortic valve implantation: first experiences in a pre-clinical model. JACC Cardiovasc Interv 2012;5:874–83.

[15] Weber B, Emmert MY, Behr L, Schoenauer R, Brokopp C, Drögemüller C. Prenatally engineered autologous amniotic fluid stem cell-based heart valves in the fetal circulation. Biomaterials 2012;33:4031–43.
[16] Schmidt D, Dijkman PE, Driessen-Mol A, Stenger R, Mariani C, Puolakka A, et al. Minimally-invasive implantation of living tissue engineered heart valves: a comprehensive approach from autologous vascular cells to stem cells. J Am Coll Cardiol 2010;56:510–20.
[17] Weber B, Scherman J, Emmert MY, Gruenenfelder J, Verbeek R, Bracher M, et al. Injectable living marrow stromal cell-based autologous tissue engineered heart valves: first experiences with a one-step intervention in primates. Eur Heart J 2011;32:2830–40.
[18] Weber B, Falk V, Hoerstrup SP. Cardiovascular in situ tissue engineering. Cardiovasc Med 2012;15:339–44.
[19] Dijkman PE, Driessen-Mol A, Frese L, Hoerstrup SP, Baaijens FP. Decellularized homologous tissue-engineered heart valves as off-the-shelf alternatives to xeno- and homografts. Biomaterials 2012;33:4545–54.
[20] Mol A, van Lieshout MI, Dam-de Veen CG, Neuenschwander S, Hoerstrup SP, Baaijens FP, et al. Fibrin as a cell carrier in cardiovascular tissue engineering applications. Biomaterials 2005;26:3113–21.
[21] Mol A, Driessen NJ, Rutten MC, Hoerstrup SP, Bouten CV, Baaijens FP. Tissue engineering of human heart valve leaflets: a novel bioreactor for a strain-based conditioning approach. Ann Biomed Eng 2005;33:1778–88.
[22] Cesarone CF, Bolognesi C, Santi L. Improved microfluorometric DNA determination in biological material using 33258 Hoechst. Anal Biochem 1979;100:188–97.
[23] Farndale RW, Buttle DJ, Barrett AJ. Improved quantitation and discrimination of sulphated glycosaminoglycans by use of dimethylmethylene blue. Biochim Biophys Acta 1986;883:173–7.
[24] Huszar G, Maiocco J, Naftolin F. Monitoring of collagen and collagen fragments in chromatography of protein mixtures. Anal Biochem 1980;105:424–9.
[25] David C, Nöhammer B, Solak H, Ziegler E. Differential X-ray phase contrast imaging using a shearing interferometer. Appl Phys Lett 2002;81:3287–9.
[26] Weitkamp T, Diaz A, David C, Pfeiffer F, Stampanoni M, Cloetens P, et al. X-ray phase imaging with a grating interferometer. Opt Express 2005;13:6296–304.
[27] Pfeiffer F, Bunk O, David C, Bech M, Le Duc G, Bravin A, et al. High-resolution brain tumor visualization using three-dimensional x-ray phase contrast tomography. Phys Med Biol 2007;52:6923–30.
[28] McDonald SA, Marone F, Hintermüller C, Mikuljan G, David C, Pfeiffer F, et al. Advanced phase-contrast imaging using a grating interferometer. J Synchrotron Radiat 2009;16:562–72.
[29] Modregger P, Pinzer BR, Thüring T, Rutishauser S, David C, Stampanoni M. Sensitivity of X-ray grating interferometry. Opt Express 2011;19:18324–38.
[30] Stark J. The use of valved conduits in pediatric cardiac surgery. Pediatr Cardiol 1998;19:282–8.
[31] Hoerstrup SP, Cummings I, Lachat M, Schoen FJ, Jenni R, Leschka S, et al. Functional growth in tissue-engineered living, vascular grafts: follow-up at 100 weeks in a large animal model. Circulation 2006;114:I159–66.
[32] Brennan MP, Dardik A, Hibino N, Roh JD, Nelson GN, Papademitris X. Tissue-engineered vascular grafts demonstrate evidence of growth and development when implanted in a juvenile animal model. Ann Surg 2008;248:370–7.
[33] van Vlimmeren MA, Driessen-Mol A, Oomens CW, Baaijens FP. Passive and active contributions to generated force and retraction in heart valve tissue engineering. Biomech Model Mechanobiol 2012;11:1015–27.
[34] van Vlimmeren MA, Driessen-Mol A, Oomens CW, Baaijens FP. An in vitro model system to quantify stress generation, compaction, and retraction in engineered heart valve tissue. Tissue Eng Part C Methods 2011;17:983–91.
[35] Walker GA, Masters KS, Shah DN, Anseth KS, Leinwand LA. Valvular myofibroblast activation by transforming growth factor-beta: implications for pathological extracellular matrix remodeling in heart valve disease. Circ Res 2004;95:253–60.
[36] Armstrong EJ, Bischoff J. Heart valve development: endothelial cell signaling and differentiation. Circ Res 2004;95:459–70.